Materials Today: Proceedings 67 (2022) 368–371

Contents lists available at ScienceDirect

Materials Today: Proceedings

journal homepage: www.elsevier.com/locate/matpr

Mechanical alloying and amorphization of $Ti_{75}Cu_{25}$ alloy

P. Urban [a,*], R. Astacio [a], R.M. Aranda [b], F. Ternero [a], J. Cintas [a]

[a] Advanced Materials Engineering Group, Escuela Técnica Superior de Ingeniería, Universidad de Sevilla, 41092 Sevilla, Spain
[b] Advanced Materials Engineering Group, Escuela Técnica Superior de Ingeniería, Universidad de Huelva, 21071 Huelva, Spain

ARTICLE INFO

Article history:
Available online 26 July 2022

Keywords:
Titanium
Copper
Powder
Metallurgy
Amorphization
Mechanical alloying

ABSTRACT

Ti-Cu alloys are used in dental and medical applications, due to their good mechanical properties, corrosion resistance and antibacterial properties. These properties are sensitive to microstructure and can be improved by formation of intermetallic compounds or amorphization of crystalline Ti-Cu powder. This study focuses on the amorphization of $Ti_{75}Cu_{25}$ powders prepared by mechanical alloying (MA). Ball milling, up to 60 h, of Ti and Cu powders leads to an amorphous structure. Laser granulometry, X-ray diffraction (XRD), scanning electron microscopy (SEM), and transmission electron microscopy (TEM) were carried out for different milling times. Future research on consolidation of amorphous powder via electrical resistance sintering will be performed to obtain bulk samples with amorphous phase and/or nanocrystalline phase with Ti_3Cu and/or Ti_2Cu intermetallic compounds.

1. Introduction

Crystalline alloys based on Ti-Cu have industrial interest due to their good corrosion resistance [1,2] and good mechanical [3,4], thermal [5] and antibacterial properties [6,7]. The most widespread applications in recent years of crystalline alloys based on Ti-Cu are dental biomedical and implant applications [8,9]. Some properties (mechanical [10], magnetic [11]) of crystalline alloys can be improved by amorphizing the crystalline phase, resulting in an amorphous alloy with long-range disorder. Additionally, the composition (Ti-25 at.% Cu) can lead to the formation of intermetallic Ti_2Cu and/or Ti_3Cu compounds (after the consolidation of amorphous powder), with good antibacterial properties [12,13]. The best-known processes to amorphize the crystalline phase are melt spinning [14] and mechanical alloying [15]. Melt spinning is a technique that is used for extremely rapid liquid cooling. It consists of a metallic wheel that is internally cooled, usually with water or liquid nitrogen, and rotates at high speed. A thin jet of liquid is injected at high pressure on the outer surface of the wheel and cooled, causing extremely rapid solidification. Cooling velocities can be achieved between 10^4 and 10^7 Kelvins per second. Mechanical alloying consists of an axis rotating in a cylindrical vial. The cylindrical vial is partially filled with balls that hit and deform metallic powder particles. In this way, the powder is plastically deformed and the crystalline structure is gradually converted into an amorphous one. In the case of Ti-Cu-based alloys, different types of amorphization processes have been developed, such as melt spinning [16–18], sputtering [19], cold rolling [20], or mechanical alloying [21,22].

2. Experimental procedure

In all experiments, pure crystalline Ti grade T-N4 (SE-JONG Materials Co. ltd, purity 99.0%, average particle size 18 ± 3 μm) and Cu CH-10L (Sigma-Aldrich, purity 99.5%, particle size <425 μm) powders were used. The desired $Ti_{75}Cu_{25}$ alloy has been achieved by mixing 75 at.% of Ti and 25 at.% of Cu. The mechanical alloy process (Fig. 1) was carried out as follows: 72 g of $Ti_{75}Cu_{25}$ was poured and hermetically sealed in a cylindrical vessel with stainless steel balls. It has been added 1.5 wt% of wax ($H_{76}C_{38}O_2N_2$) to avoid welding between metallic powder and balls and the vessel. The entire set was milled for 60 h in an argon atmosphere to avoid oxidation and refrigerated at a temperature of 25 °C to avoid possible phase transformations. The rotating impeller turned 500 rpm and the weight ratio between the milling balls and the powder was around 50:1. The entire milling process was interrupted in 1, 5, 10, 15, 20, 30, 40, 50 and 60 h to remove a small amount of powder for subsequent determination of particle size, microstructural characterization, and phase analysis. To describe

* Corresponding author.
E-mail address: purban@us.es (P. Urban).

https://doi.org/10.1016/j.matpr.2022.07.214
2214-7853/

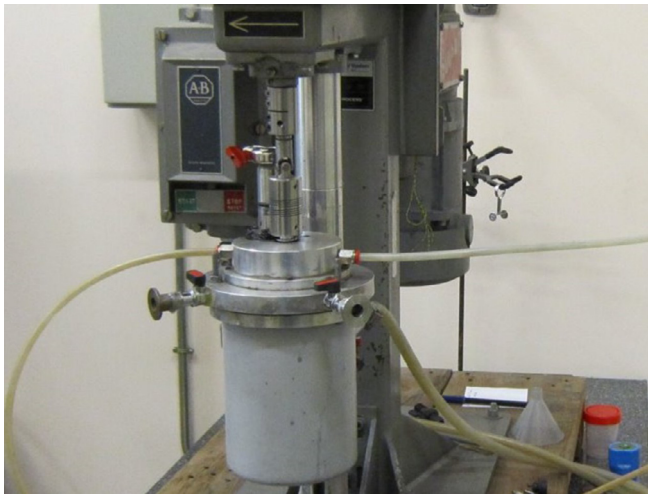

Fig. 1. Mechanical alloying process.

the microstructural evolution over the time of milling and to determine if the alloy has been amorphized, the following characterization methods have been done: laser diffraction granulometry by Mastersizer 2000, X-ray diffraction by XRD Siemens D500, scanning electron microscopy by SEM Philips XL 30 and transmission electron microscopy by TEM Philips CM-200.

3. Results and discussion

3.1. Laser diffraction granulometry

The results of laser diffraction granulometry of the $Ti_{75}Cu_{25}$ alloy during different milling stages of the MA process are shown in Fig. 2. The average particle size D(0.5) of pure titanium and pure copper are approximately 28.3 and 33.7 μm, respectively. The mixture of $Ti_{75}Cu_{25}$ has D(0.5) of approximately 29.6 μm. During the first hour of milling, the ductile titanium and copper particles undergo welding and their D(0.5) increases to about 48.9 μm. The increase of D(0.5) continues for 5 h of milling with 53.4 μm. After 5 h of milling, the particles are hardened and D(0.5) begins to decrease. For 10 h milling, D(0.5) decreases to 37.3 μm. Finally, as the milling time increases, D(0.5) decreases to about 6.2 μm after milling for 60 h milling.

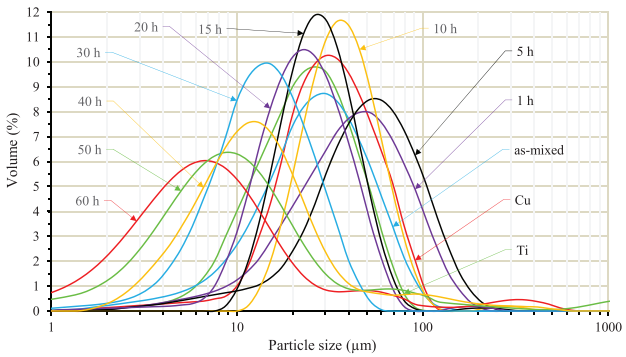

Fig. 2. Laser diffraction granulometry of $Ti_{75}Cu_{25}$ as-mixed powders and powders milled at different times.

3.2. Scanning electron microscopy

The results of scanning electron microscopy of the $Ti_{75}Cu_{25}$ alloy during different milling stages of the MA process are shown in Fig. 3. In Fig. 3a, the backscattered electron micrograph (BSE) of the pure titanium and pure copper mixture is shown. Particles of irregular and dendritic form belong to titanium and copper,

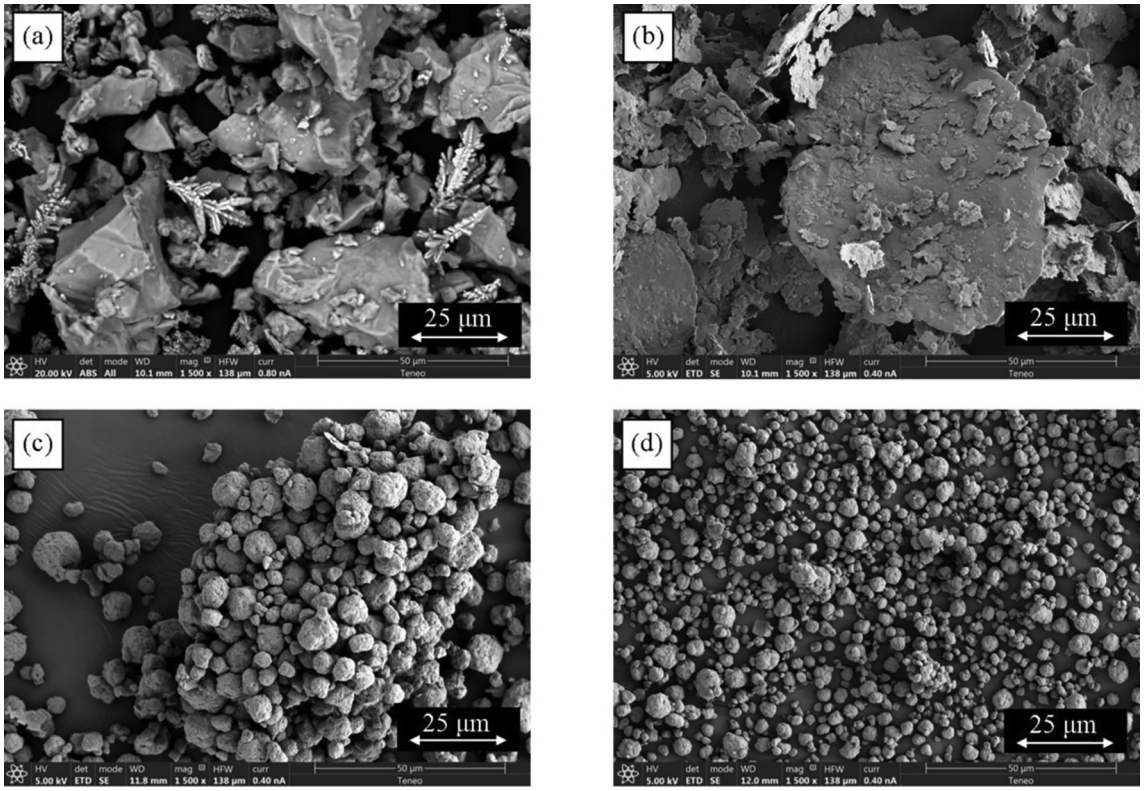

Fig. 3. SEM image of $Ti_{75}Cu_{25}$ (a) as-mixed powders and powders milled for (b) 1, (c) 20 and (d) 60 h.

respectively. In Fig. 3b–d, the secondary electron micrographs (SE) of the $Ti_{75}Cu_{25}$ alloy are shown. After 1 h of milling (Fig. 3b), the titanium and copper particles are crushed and suffer plastic deformation due to the shocks of the balls. The particles suffer welding, their size increases, and the shape of the particles flattens. After 20 h of milling (Fig. 3c), the particles harden and preferably suffer fragmentation due to their fragile character. With increasing milling time, the particle size continues to decrease until 60 h of milling (Fig. 3d).

3.3. X-ray diffraction

The results of the X-ray diffraction of the $Ti_{75}Cu_{25}$ alloy during different milling stages of the MA process are shown in Fig. 4. The X-ray diffraction pattern of the mixture of pure titanium and pure copper powders shows narrow peaks with high intensities. With the increase of the milling times, the crystalline peaks begin to broaden as a result of decreases in the crystallite size, and the intensities of the elemental crystalline diffraction peaks are reduced. After 20 h of milling, the diffraction pattern has only one broad diffuse peak with a maximum at $2\Theta = 40°$, indicating that the elemental powder mixture has transformed into a nanocrystalline and/or amorphous phase. The diffraction patterns of the powders milled for longer times do not show any appreciable changes.

3.4. Transmission electron microscopy

The results of transmission electron microscopy of the $Ti_{75}Cu_{25}$ alloy during different milling stages of the MA process are shown

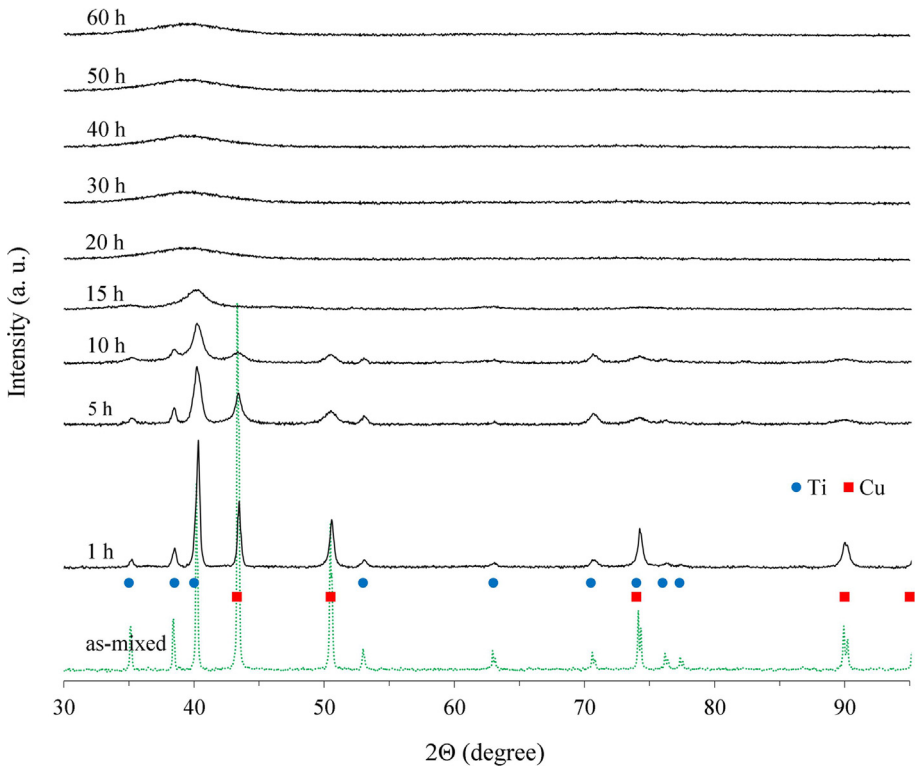

Fig. 4. XRD patterns of the $Ti_{75}Cu_{25}$ alloy milled for different milling times.

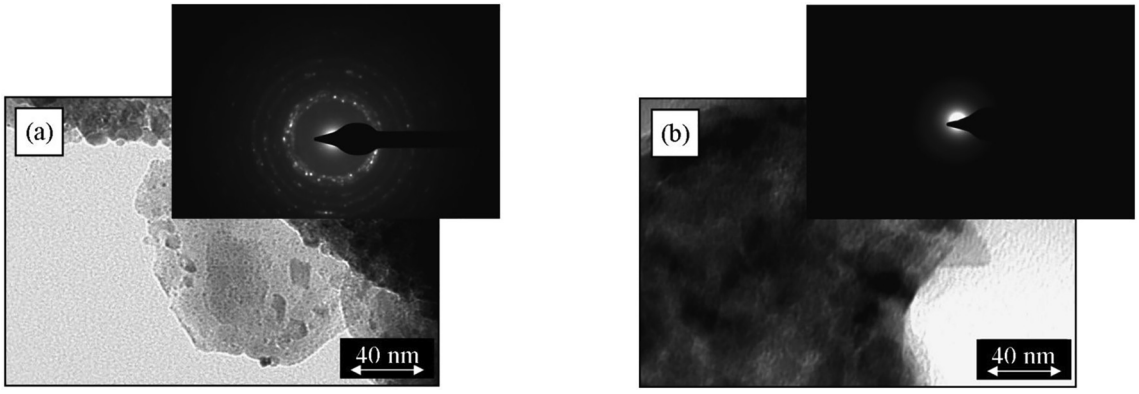

Fig. 5. TEM image and selected area diffraction pattern of $Ti_{75}Cu_{25}$ alloy milled for (a) 15 and (b) 60 h showing (a) nanocrystalline and crystalline phase and (b) amorphous phase.

in Fig. 5. Fig. 5a shows the powder milled for 15 h. The presence of a nanocrystalline phase can be observed with rests of the crystalline phase. After 60 h of milling (Fig. 5b), the crystalline and nanocrystalline phases completely disappear by transforming into an amorphous phase.

4. Conclusions

Mechanical alloying has been used for 60 h to amorphize the crystalline powder of $Ti_{75}Cu_{25}$. The size of the particles has decreased during milling from approximately 29.6 μm for the pure titanium and copper mixture to 6.2 μm in the case of powders milled for 60 h. The form of the particles before milling was irregular and dendritic for titanium and copper, respectively. However, the shape of the particles after 60 h of milling was spherical. X-ray diffraction has shown that narrow peaks with high intensities for the mixture disappear completely after 20 h of milling. Between 20 and 60 h of milling the diffractograms have only one wide low intensity peak with maximum at $2\theta = 40^\circ$ that belongs to the nanocrystalline and/or amorphous phase. After 15 h of milling, the presence of a nanocrystalline and crystalline phase has been proven by transmission electron microscopy. After 60 h, the powder is amorphized and no nanocrystalline or crystalline phase is observed.

Data availability

No data was used for the research described in the article.

Declaration of Competing Interest

The authors declare that they have no known competing financial interests or personal relationships that could have appeared to influence the work reported in this paper.

Acknowledgments

The authors also thank the technicians J. Pinto, M. Madrid, and M. Sánchez (University of Seville, Spain) for experimental assistance.

Funding

This research was funded by the Ministerio de Economía y Competitividad (Spain) and Feder (EU) through the research projects DPI2015-69550-C2-1-P and DPI2015-69550-C2-2-P.

References

[1] J. Wang, S. Zhang, Z. Sun, H. Wang, L. Ren, K. Yang, Optimization of mechanical property, antibacterial property and corrosion resistance of Ti-Cu alloy for dental implant, J. Mater. Sci. Technol. 35 (10) (2019) 2336–2344, https://doi.org/10.1016/j.jmst.2019.03.044.

[2] E. Zhang, X. Wang, M. Chen, B. Hou, Effect of the existing form of Cu element on the mechanical properties, bio-corrosion and antibacterial properties of Ti-Cu alloys for biomedical application, Mater. Sci. Eng., C 69 (2016) 1210–1221, https://doi.org/10.1016/j.msec.2016.08.033.

[3] W. Liu, X. Chen, T. Ahmad, C. Zhou, X. Xiao, H. Wang, B. Yang, Microstructures and mechanical properties of Cu–Ti alloys with ultrahigh strength and high ductility by thermo-mechanical treatment, Mater. Sci. Eng., A 835 (2022) 142672, https://doi.org/10.1016/j.msea.2022.142672.

[4] Y. Yuan, R. Luo, J. Ren, L. Zhang, Y. Jiang, Z. He, Design of a new Ti-Mo-Cu alloy with excellent mechanical and antibacterial properties as implant materials, Mater. Lett. 306 (2022) 130875, https://doi.org/10.1016/j.matlet.2021.130875.

[5] C. Machio, M.N. Mathabathe, A.S. Bolokang, A comparison of the microstructures, thermal and mechanical properties of pressed and sintered Ti–Cu, Ti–Ni and Ti–Cu–Ni alloys intended for dental applications, J. Alloys Compd. 848 (2020) 156494, https://doi.org/10.1016/j.jallcom.2020.156494.

[6] C. Xin, N. Wang, Y. Chen, B. He, Q. Zhao, L. Chen, Y. Tang, B. Luo, Y. Zhao, X. Yang, Biological corrosion behaviour and antibacterial properties of Ti-Cu alloy with different Ti2Cu morphologies for dental applications, Mater. Des. 215 (2022) 110540, https://doi.org/10.1016/j.matdes.2022.110540.

[7] J. Hu, H. Li, X. Wang, L. Yang, M. Chen, R. Wang, G. Qin, D.-F. Chen, E. Zhang, Effect of ultrasonic micro-arc oxidation on the antibacterial properties and cell biocompatibility of Ti-Cu alloy for biomedical application, Mater. Sci. Eng., C 115 (2020) 110921, https://doi.org/10.1016/j.msec.2020.110921.

[8] L. Bolzoni, F. Yang, Development of Cu-bearing powder metallurgy Ti alloys for biomedical applications, J. Mech. Behav. Biomed. Mater. 97 (2019) 41–48, https://doi.org/10.1016/j.jmbbm.2019.05.014.

[9] M.R. Akbarpour, S.M. Javadhesari, Wear performance of novel nanostructured Ti-Cu intermetallic alloy as a potential material for biomedical applications, J. Alloys Compd. 699 (2017) 882–886, https://doi.org/10.1016/j.jallcom.2017.01.020.

[10] P. Urban, F. Ternero, E.S. Caballero, S. Nandyala, J.M. Montes, F.G. Cuevas, Amorphous Al-Ti Powders Prepared by Mechanical Alloying and Consolidated by Electrical Resistance Sintering, Metals 9 (11) (2019) 1140–1153, https://doi.org/10.3390/met9111140.

[11] L. Guo, S. Geng, Z. Yan, Q. Chen, S. Lan, W. Wang, Nanocrystallization and magnetic property improvement of $Fe_{78}Si_9B_{13}$ amorphous alloys induced by magnetic field assisted nanosecond pulsed laser, Vacuum 199 (2022) 1–11, https://doi.org/10.1016/j.vacuum.2022.110983.

[12] Z. Zhao, W. Xu, H. Xin, F. Yu, Microstructure, corrosion and anti-bacterial investigation of novel Ti-xNb-yCu alloy for biomedical implant application, J. Mater. Res. Technol. 18 (2022) 5212–5225, https://doi.org/10.1016/j.jmrt.2022.04.1.

[13] C. Xin, N. Wang, Y. Chen, B. He, Q. Zhao, L. Chen, Y. Tang, B. Luo, Y. Zhao, X. Yang, Biological corrosion behaviour and antibacterial properties of Ti-Cu alloy with different Ti_2Cu morphologies for dental application, Mater. Des. 215 (2022) 1–11, https://doi.org/10.1016/j.matdes.2022.110540.

[14] R.M. Aranda, R. Astacio, F. Ternero, P. Urban, F.G. Cuevas, Structure and Size Distribution of Powders Produced from Melt-Spun Fe-Si-B Ribbons, Key Eng. Mater. 876 (2021) 25–30, https://doi.org/10.4028/www.scientific.net/KEM.876.25.

[15] P. Urban, F. Ternero, R.M. Aranda, R. Astacio, F.J. Cintas, Solid State Amorphization of $Ti_{60}Si_{40}$ Alloy via Mechanical Alloying, Key Eng. Mater. 876 (2021) 7–12, https://doi.org/10.4028/www.scientific.net/KEM.876.7.

[16] D.V. Gunderov, E.V. Boltynjuk, E.V. Ubyivovk, A.V. Lukyanov, A.A. Churakova, A. R. Kilmametov, Y.S. Zamula, R.Z. Valiev, Cluster structure in amorphous Ti-Ni-Cu alloys subjected to high-pressure torsion deformation, J. Alloys Compd. 749 (2018) 612–619, https://doi.org/10.1016/j.jallcom.2018.03.357.

[17] Z. Dan, F. Qin, Y. Sugawara, I. Muto, N. Hara, Fabrication of nanoporous copper by dealloying amorphous binary Ti–Cu alloys in hydrofluoric acid solutions, Intermetallics 29 (2012) 14–20, https://doi.org/10.1016/j.intermet.2012.04.016.

[18] W. Fuxiang, G. He, S. Yanwei, O. Jiqiu, H. Yezeng, M. Qingkun, Effect of Si on the Microstructure and Performance of Ti-Cu-Zr-Ni-based Amorphous Filler Metal, Rare Metal Mater. Eng. 47 (7) (2018) 2023–2027, https://doi.org/10.1016/S1875-5372(18)30175-9.

[19] H. Turnow, H. Wendrock, S. Menzel, T. Gemming, J. Eckert, Structure and properties of sputter deposited crystalline and amorphous Cu–Ti films, Thin Solid Films 598 (2016) 184–188, https://doi.org/10.1016/j.tsf.2015.10.081.

[20] G.P. Dinda, H. Rösner, G. Wilde, Cold-rolling induced amorphization in Cu–Zr, Cu–Ti–Zr and Cu–Ti–Zr–Ni multilayers, J. Non-Cryst. Solids 353 (32–40) (2007) 3777–3781, https://doi.org/10.1016/j.jnoncrysol.2007.05.147.

[21] L.C. Zhang, K.B. Kim, P. Yu, W.Y. Zhang, U. Kunz, J. Eckert, Amorphization in mechanically alloyed (Ti, Zr, Nb)–(Cu, Ni)–Al equiatomic alloys, J. Alloys Compd. 428 (1–2) (2007) 157–163, https://doi.org/10.1016/j.jallcom.2006.03.092.

[22] C. Chen, R.D. Ding, X.M. Feng, Y.F. Shen, Fabrication of Ti–Cu–Al coatings with amorphous microstructure on Ti–6Al–4V alloy substrate via high-energy mechanical alloying method, Surf. Coat. Technol. 236 (2013) 485–499, https://doi.org/10.1016/j.surfcoat.2013.10.043.